Photochemical & Photobiological Sciences

Accepted Manuscript

This is an *Accepted Manuscript*, which has been through the Royal Society of Chemistry peer review process and has been accepted for publication.

Accepted Manuscripts are published online shortly after acceptance, before technical editing, formatting and proof reading. Using this free service, authors can make their results available to the community, in citable form, before we publish the edited article. We will replace this *Accepted Manuscript* with the edited and formatted *Advance Article* as soon as it is available.

You can find more information about *Accepted Manuscripts* in the Information for Authors.

Please note that technical editing may introduce minor changes to the text and/or graphics, which may alter content. The journal's standard Terms & Conditions and the Ethical guidelines still apply. In no event shall the Royal Society of Chemistry be held responsible for any errors or omissions in this *Accepted Manuscript* or any consequences arising from the use of any information it contains.

ROYAL SOCIETY OF CHEMISTRY

www.rsc.org/pps

Journal Name RSCPublishing

ARTICLE

Lophine derivatives as activators in peroxyoxalate chemiluminescence

Cite this: DOI: 10.1039/x0xx00000x

Received 00th January 2012, Accepted 00th January 2012

DOI: 10.1039/x0xx00000x

www.rsc.org/

J. Alves,[a] A. Boaro,[a] J. S. da Silva,[b] T. L. Ferreira,[b] V. B. Keslarek,[a] C. A. Cabral,[a] R. B. Orfão Jr.,[a] L. F. M. L. Ciscato[a] and F. H. Bartoloni*,[a]

Lophine and four of its derivatives were used as activators (ACTs) of the chemiluminescent peroxyoxalate (PO) reaction of bis(2,4,6-trichlorophenyl)oxalate with H_2O_2, catalysed by imidazole. Kinetic emission assays have shown that with the tested compounds the reaction mechanism, regarding the formation of the High Energy Intermediate (HEI) of the PO reaction, occurs as previously seen for commonly used ACTs. A bimolecular interaction of the compounds with the HEI leads to chemiexcitation through the Chemically Initiated Electron Exchange Luminescence (CIEEL) mechanism, as confirmed by a linear free-energy correlation between the relative catalytic rate constants and the oxidation potentials of the compounds. The yields of excited state formation and light emission, in the range of 10^{-2} to 10^{-3} E mol^{-1}, are comparable to the ones seen with commonly used ACTs. A Hammett plot with ρ = –0.90 indicates the build up of a partial positive charge on the transition step of the catalytic process, consistent with the formation of a radical cation of the ACT, being an additional validation of the CIEEL mechanism in this system.

Introduction

Chemiluminescence (CL) is the emission of light as one of the products of a chemical transformation. One of the first CL reactions to be described was the autooxidation of lophine (**1**), reported by Radziszewski in 1877,[1] who observed a yellow emission from its reaction with oxygen in the presence of a strong base. The reaction mechanism (**Scheme 1**) involves the oxidation of lophine by oxygen, leading to a hydroperoxide, which then forms a 1,2-dioxetane intermediate by cyclization.[2] Finally, the decomposition of this unstable cyclic peroxide leads to the electronic excited state of an amidine, which decays to the fundamental state emitting light.[2]

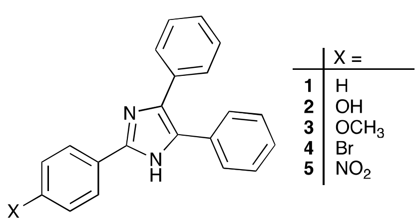

Due to the CL and fluorescent properties of lophine and its derivatives, much has been done in using them in analytical systems combining HPLC and FIA techniques, for the determination of trace amounts of inorganic and organic compounds.[3] Nowadays, the attention received by lophine and its derivatives is given specially due to their use as fluorescent labels for amines, phenols and carboxylic acids.[3] Nonetheless, new features have been developed with focus on its CL properties, for example, applying lophine as an enhancer for the classical luminol CL reaction.[4]

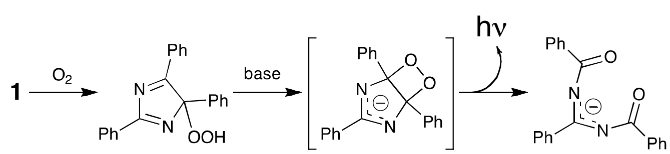

Scheme 1 Mechanism for the classical lophine chemiluminescence pathway, through a 1,2-dioxetane-like intermediate, furnishing an amidine and light as products.

To expand the use of lophine derivatives, we have applied compounds **1**–**5** in other CL system, the *peroxyoxalate reaction* (PO, **Scheme 2**);[5,6] these substituted lophines were used as *activators* (ACTs) of this CL transformation,[6] therefore, the mechanism of excited states generation is completely different from the one involving a 1,2-dioxetane, as described in **Scheme 1**. As a matter of fact, in the PO system an electron transfer (ET) takes place from the ACT to the high-energy intermediate (HEI),[6-9] the later being generated on a previous reaction between an oxalic ester and H_2O_2, catalysed by base (see below).[10] Since an ET is proven to occur in the PO system, the use of lophine derivatives as activators allows one to probe the influence of different substituents with electron-donating and -withdrawing properties on a common structural motif, *i.e.* the 2,4,5-triphenylimidazole system.

Photochemical & Photobiological Sciences Accepted Manuscript

The peroxyoxalate (PO) reaction

The reaction between bis(2,4,6-trichlorophenyl)oxalate (TCPO) and H_2O_2 catalysed by imidazole (IMI-H) was studied in depth by Stevani *et al.*[10] Several polycondensed aromatic hydrocarbons (PAH), such as rubrene, perylene and anthracene derivatives were used as ACTs, due to their high fluorescence quantum yields (Φ_{FL}) and low oxidation potentials (E^{ox}).[6] The mechanism for such transformation can be summarized as follows (**Scheme 2**):[7,10] imidazole act as a nucleophilic catalyst leading to the formation of an 1,1'-oxalyldiimidazolic intermediate (step 1); H_2O_2 performs a nucleophilic attack on such intermediate, forming a peroxalic acid (step 2); this peroxide undergoes a cyclization, leading to the PO reaction HEI, the 1,2-dioxetanedione (step 3);[7] in the last step, the chemiexcitation process occurs through a bimolecular interaction between the peroxidic HEI and the ACT (step 4); steps 1 to 3 can all occur with IMI-H acting as a basic catalyst.

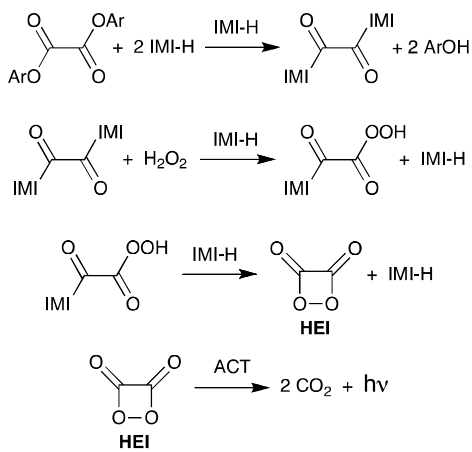

Scheme 2 PO mechanism in EtOAc, as described by da Silva *et al.* and Stevani *et al.* (for TCPO, ArOH = 2,4,6-trichlorophenol).[7,10]

The rate-limiting steps in such transformation are steps 1 and 2 (occasionally step 3, but only at high concentrations of H_2O_2)[10] and, thus, are the ones observable through CL kinetic measurements, when light emission time profiles are recorded. As depicted in **Scheme 3**, the HEI can decompose unimolecularly generating two CO_2 molecules without light production. This process has a k_D rate constant addressed to it, that competes with the HEI-ACT bimolecular interaction.

The chemiexcitation step

The bimolecular interaction between the HEI and the ACT (**Scheme 2**, step 4) is responsible for the chemiexcitation process. Such catalysed decomposition is believed to occur through the Chemically Initiated Electron Exchange Luminescence mechanism (CIEEL).[6,11] Indeed, the CIEEL mechanism has been successfully used to rationalize results regarding an initial ET in many studies with the PO reaction.[8,9]

The whole process of light generation (**Scheme 2**, step 4) can be summarized as follows (**Scheme 3**): the ACT-catalysed decomposition of the HEI – described by a k_{CAT} rate constant – involves an ET from the ACT to the HEI, leading to the formation of the radical ions $ACT^{\bullet+}$ and $HEI^{\bullet-}$. This ET is actually accompanied by a concerted O–O bond cleavage (see below, **Scheme 4**). The $HEI^{\bullet-}$ radical anion decomposes eliminating a CO_2 molecule due to the rupture of the C–C bond, generating the carbon dioxide radical anion, *i.e.* $CO_2^{\bullet-}$. An electron-back transfer (EBT) ensues in the annihilation of the $CO_2^{\bullet-}$ and $ACT^{\bullet+}$ radical ions, a highly exergonic process that is capable of generating the ACT molecule on the singlet excited state (ACT*). Finally, the ACT* molecule emits light through a fluorescent decay.

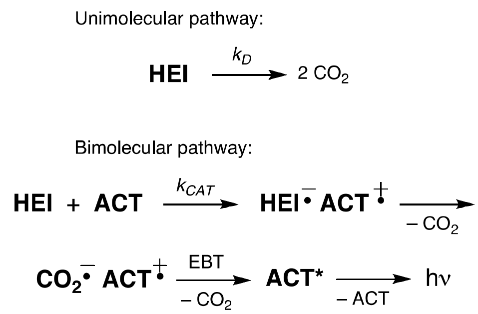

Scheme 3 HEI consumption pathways; (top) unimolecular decomposition without light generation; (bottom) bimolecular ACT-catalysed decomposition, through the light emitting-CIEEL mechanism.

Since the use of lophine and its derivatives as ACTs of the peroxyoxalate reaction is proposed here, it is recommended that CL kinetic assays are performed to address: *(i)* if the overall mechanism for IAE formation is the same as with commonly used ACTs, and *(ii)* confirm the initial ET occurring at the chemiexcitation step, as predicted by the CIEEL sequence.

Experimental

General materials and procedures

Ethyl acetate (EtOAc, Sigma-Aldrich, ACS reagent, ≥99.5%), imidazole (IMI-H, Sigma, ACS reagent, ≥99% by titration, crystalline), bis(2,4,6-trichlorophenyl)oxalate (TCPO, Sigma, BioReagent, suitable for chemiluminescence, ≥99.0%), hexane (Synth, analytical grade), benzaldehyde (Sigma-Aldrich, ≥99%), 4-hydroxybenzaldehyde (Aldrich, 98%), 4-anisaldehyde (Aldrich, 98%), 4-bromobenzaldehyde (Sigma-Aldrich, 99%), 4-nitrobenzaldehyde (Aldrich, 98%), benzil (Aldrich, 98%), ammonium acetate (Sigma-Aldrich, reagent grade, ≥98%) and acetic acid (Sigma-Aldrich, Reagent Plus, ≥99%) were used as received. Deionized water was obtained through a Milli-Q Millipore purifying system (conductivity 18.2 MΩ cm). Quartz cuvettes (Hellma, QS Suprasil) had a volume of 3.0 mL and an optical path of 10.00 mm, with two polished sides for absorption assays and four sides for fluorescence or chemiluminescence assays. Small sample volumes (μL) were transferred through Hamilton microsyringes. H_2O_2 stock solutions were prepared diluting a 60% aqueous solution (Solvay Peróxidos do Brasil Ltda.) in EtOAc, the residual water being removed by the addition of

This journal is © The Royal Society of Chemistry 2012
Photochemical & Photobiological Sciences Accepted Manuscript

$MgSO_4$ followed by filtration; the final H_2O_2 concentration was determined iodometrically.[12]

Equipment

UV-Vis absorption spectra were recorded on a Varian Cary 60 with a multicell holder thermostatized at 25 °C by a Varian Cary PCB 1500 system. Fluorescence spectra were recorded on a Varian Cary Eclipse with a single-cell holder thermostatized by a Varian Cary PCB 1500 system; kinetic chemiluminescence assays were performed on the same spectrophotometer, with the excitation lamp turned off and collecting all the wavelengths emitted by the sample. CHN composition was obtained in a Perkin-Elmer CHN 2400 analyzer, using benzoic acid as standard. NMR spectra were obtained at 25 °C on a Bruker AIII 300 or 500 MHz spectrometer; chemical shifts (δ) are reported in parts per million (ppm) relative to tetramethylsilane (TMS); coupling constant *J* values are given in Hz. Cyclic voltammograms where acquired on an Autolab PGSTAT 128N potentiostat/galvanostat equipped with a module for low currents, using a conventional electrochemical cell consisting of reference electrode (Ag|AgCl, concentrated KCl), auxiliary electrode (Pt) and working electrode (microelectrode Pt disc with a 65 μm radius), in dimethylsulfoxide (DMSO) as solvent and with tetrabultylammonium perchlorate (0.1 mol L^{-1}) as electrolyte. Half-wave oxidation potentials (E^{ox}) where obtained from the current value corresponding to half of the limiting current, and converted to saturated calomel electrode (SCE).

Lophine derivatives 1–5

The known compounds **1**–**5** were prepared following a general procedure based on Benisvy *et al.*[13] A 100 mL single-neck round-bottomed flask was charged with a mixture of the substituted benzaldehyde (8.8 mmol), benzil (8.6 mmol) and ammonium acetate (32 mmol), in 30 mL of glacial acetic acid. A reflux condenser was set up and the solution was kept under reflux for 2 to 3 hours; in some cases, the formation of a precipitate was observed. Afterwards, 50 mL of ice-cold deionized water were added, forcing the precipitation of the lophine; the crude product was collected by filtration, washed with water (5 × 15 mL) and dried by suction. The resulting solid was dissolved in EtOAc and dried over $MgSO_4$. The solution was filtered and the solvent removed by rotary evaporation, yielding a solid that was purified by recrystallization from EtOAc or EtOAc/hexane.

2,4,5-Triphenyl-1*H*-imidazole (lophine, 1). 1.85 g of a white colored cotton-like solid (71%). Found: C, 84.5; H, 5.4; N, 9.3; Calc. for $C_{21}H_{16}N_2$: C, 85.1; H, 5.4; N, 9.5%. δ_H (300 MHz; DMSO-d^6) 7.3-7.6 (13 H, m, ArH), 8.1 (2 H, d, *J* = 7.2 Hz, ArH), 12.7 (1 H, br s, NH). δ_C (75 MHz; DMSO-d^6) 125.22, 126.50, 127.21, 128.27, 128.46, 128.71, 130.37, 131.05, 135.28, 137.11, 145.54.

2-(4-Hydroxyphenyl)-4,5-diphenyl-1*H*-imidazole (2). 1.33 g of slightly yellow crystals (48%). Found: C, 80.4; H, 5.3; N, 8.8; Calc. for $C_{21}H_{16}N_2O$: C, 80.8; H, 5.2; N, 9.0%. δ_H (500 MHz; DMSO-d^6) 5.97 (2 H, dt, *J* = 8.7 and 2.7 Hz, ArH), 6.3-6.7 (10 H, m, ArH), 7.02 (2 H, dt, *J* = 8.7 and 2.7 Hz, ArH), 8.83 (1 H, br s, ArOH), 11.52 (1 H, br s, NH). δ_C (125 MHz; DMSO-d^6) 18.54, 56.01, 115.37, 121.63, 126.31, 126.81, 127.01, 127.33, 127.49, 128.10, 128.29, 128.58, 131.30, 135.41, 136.57, 146.03, 157.75.

2-(4-Methoxyphenyl)-4,5-diphenyl-1*H*-imidazole (3). 1.41 g of a white solid (50%). Found: C, 80.9; H, 5.5; N, 8.5; Calc. for $C_{22}H_{18}N_2O$: C, 80.9; H, 5.6; N, 8.6%. δ_H (300 MHz; DMSO-d^6) 3.82 (3 H, s, OMe), 7.05 (2 H, d, J = 9 Hz, ArH), 7.2-7.5 (10 H, m, ArH) 8.03 (2H, d, *J* = 9 Hz, ArH), 12.5 (1 H, br s, NH). δ_C (75 MHz; DMSO-d^6) 55.28, 114.21, 123.10, 126.53, 126.71, 127.20, 127.77, 128.25, 128.51, 128.76, 131.18, 135.44, 136.70, 145.60, 159.39.

2-(4-Bromophenyl)-4,5-diphenyl-1*H*-imidazole (4). 1.01 g of a white solid (31%). Found: C, 67.9; H, 4.1; N, 7.4; Br, 21.4; Calc. for $C_{21}H_{15}N_2Br$: C, 67.2; H, 4.0; N, 7.5; Br, 21.3%. δ_H (300 MHz; DMSO-d^6) 7.37 (6H, br s, ArH), 7.53 (4 H, d, *J* = 6.9 Hz, ArH), 7.69 (2 H, d, *J* = 8.7 Hz, ArH), 8.04 (2 H, d, *J* = 8.7 Hz, ArH), 12.8 (1 H, br s, NH). δ_C (75 MHz; DMSO-d^6) 121.75, 127.59, 128.86, 129.98, 132.12, 144.93.

2-(4-Nitrophenyl)-4,5-diphenyl-1*H*-imidazole (5). 1.17 g of a deep-yellow solid (39%). Found: C, 72.9; H, 4.4; N, 12.5; Calc. for $C_{21}H_{15}N_2Br$: C, 73.9; H, 4.4; N, 12.3%. δ_H (300 MHz; DMSO-d^6) 7.10-7.25 (3 H, m, ArH), 7.30-7.40 (3 H, m, ArH) 7.47 (2 H, dd, *J* = 8 and 1.5 Hz, ArH), 7.54 (2 H, dd, *J* = 8 and 1.5 Hz, ArH), 8.2-8.38 (4 H, m, ArH). δ_C (75 MHz; DMSO-d^6) 124.05, 125.89, 126.95, 127.56, 128.21, 128.33, 128.72, 128.80, 130.25, 131.00, 134.90, 136.63, 139.01, 143.82, 146.80.

Chemiluminescence kinetic assays

All CL kinetic assays were carried out in fluorescence quartz cuvettes. To a cuvette charged with EtOAc, the desired amounts of IMI-H, H_2O_2 and ACT stock solutions (also prepared in EtOAc) were added, and the mixture was allowed to thermally equilibrate with the cell holder at 25 °C for five minutes. The reaction was started with the injection of the TCPO stock solution (prepared in EtOAc), immediately followed by data acquisition on the spectrofluorimeter. The sum of all the volumes added, from EtOAc to the reagents stock solutions, was kept constant at 3.0 mL. The reagents final concentrations were the following: *(i)* [TCPO] was kept at 0.1 mmol L^{-1} throughout all the experiments; *(ii)* when the [IMI-H] was varied (from 0.2 to 20 mmol L^{-1}), the [H_2O_2] and [ACT] were 10.0 and 1.0 mmol L^{-1}, respectively; *(iii)* when the [H_2O_2] was varied (from 0.25 to 10 mmol L^{-1}), the [IMI-H] and [ACT] were both 1.0 mmol L^{-1}; *(iv)* when the [ACT] was varied (from 0.1 to 1.0 or 10.0 mmol L^{-1}), the [IMI-H] and [H_2O_2] were 1.0 and 10.0 mmol L^{-1}, respectively. The curves of light intensity vs. time (*i.e.* CL-intensity time-profiles) were observed for at least three half-lives, and fitted by a double exponential

Photochemical & Photobiological Sciences Accepted Manuscript

equation.[8-10] Using the fitted parameters, the curve was extrapolated to zero counts and the integrated areas under the light emission curves (Q, in arbitrary units, a.u.) calculated.[8-10]

Quantum yields

Fluorescence quantum yields (Φ_{FL}) for the lophine derivatives **1**–**5** were determined using anthracene (Φ_{FL} = 0.27)[14] as a relative standard. The chemiluminescence quantum yields (Φ_{CL}, in E mol^{-1}) of the kinetic assays were determined by correcting Q, which is in arbitrary units (a.u.), by a calibration factor in E a.u.$^{-1}$ (f_{cal}, **Eq. 1**);[8] f_{cal} was determined using the luminol standard[15] under instrumental conditions identical to the ones used for the kinetic assays. Also, a correction factor for the photomultiplier's wavelength sensibility (f_{PMT}) was taken into account (**Eq. 1**). Normalization by the number of moles of the limiting reactant, which is TCPO, finally furnishes Φ_{CL} in E mol^{-1} (**Eq. 1**).[8] Singlet excited state formation quantum yields (Φ_S) were determined normalizing Φ_{CL} by Φ_{FL} (**Eq. 2**).

$$\Phi_{CL} = \frac{Q f_{cal} f_{PMT}}{n_{TCPO}} \qquad (1)$$

$$\Phi_S = \frac{\Phi_{CL}}{\Phi_{FL}} \qquad (2)$$

Results and Discussion

The PO mechanism with lophine derivatives

Lophine (**1**), as well as its derivatives **2**–**5**, are fluorescent molecules with a Φ_{FL} ~ 0.4, except for the bromo-substituted **4**; they absorb over 300 nm, with molar extinction coefficients of at least 20000 L mol^{-1} cm^{-1}, fluorescing above 380 nm (**Table 1**). Despite of being used in several analytical systems,[3] including applying the CL emission of **1** for ions detection,[16] lophine and its derivatives have never been used before as ACTs of the PO system.

Table 1. Photophysical properties of the lophine derivatives **1** – **5**.

ACT	λ_{ABS} † (nm)	ε ‡ (L mol^{-1} cm^{-1})	λ_{FL} † (nm)	Φ_{FL}	ν_{0-0} § (cm^{-1})
1	309	21400 ± 60	382	0.45	28694
2	301	25720 ± 40	391	0.39	28409
3	304	25400 ± 90	390	0.37	28490
4	316	33500 ± 20	380	0.08	28409
5	390	31600 ± 50	544	0.45	21668

† Absorption and emission maxima wavelengths. ‡ Determined as the angular coefficient of λ_{ABS} vs. concentration linear plots (**Figure S1**), setting the linear coefficient as zero; r > 0.9999 in all cases. § 0→0 transition obtained at the crossing point of absorption and emission spectra (**Figure S2**).

Before searching for evidences of an ET in the chemiexcitation process (**Scheme 3**), we verified if compounds **1**–**5** would affect the slower, rate-determining steps of the PO reaction (steps 1 and 2, **Scheme 2**), which are the ones observable kinetically. Our results will be compared to the ones found by da Silva *et al.* and Stevani *et al.*,[10] which have worked with 9,10-diphenylanthracene (DPA) to rationalize the PO mechanism in EtOAc (**Scheme 2**).

CL-intensity time-profiles were recorded for different concentrations of **1**–**5** while keeping the concentration of the other reagents constant (**Figure S3**); after fitting with a double exponential equation, values for the CL maximum intensity (I_{max}) and the rise (k_2) and fall (k_1) rate constants were determined (**Table S1**). It has been previously shown[10] that the fall rate constant k_1 corresponds to step 1, while the rise rate constant k_2 corresponds to step 2 (**Scheme 2**). k_1 and k_2 did not change with the concentration of **1**–**5** (**Table S1**), with overall averages of (3.7 ± 0.3) × 10^{-3} and (3 ± 1) × 10^{-1} s^{-1}, respectively; therefore, the kinetically observable steps 1 and 2 (**Scheme 2**) of the PO reaction are independent of the type and concentration of lophine derivative applied as ACT. Such mean values are in agreement with those found previously for DPA – k_1 = 3.5 × 10^{-3} and k_2 = 1.3 × 10^{-1} s^{-1}.[10] It is important to notice that the emitting species of the CL reaction is the fluorescent state of the compound, as seen by the clear overlay of CL and FL spectra (**Figure S4**).

CL kinetic assays were also performed varying the concentration of IMI-H or H_2O_2, while keeping the other reagents' concentration constant, using [**1**] = 1.0 mmol L^{-1} as ACT (**Tables S2** and **S3**). A quadratic relationship of k_1 with the [IMI-H] (**Eq. 3**) was observed (**Figure 1**), with bimolecular $k_{1(2)}$ and termolecular $k_{1(3)}$ rate constants of 2.4 ± 0.1 L mol^{-1} s^{-1} and (9.03 ± 0.05) × 10^2 L^2 mol^{-2} s^{-1}, which are in agreement with the ones found for DPA, of 1.4 ± 0.1 L mol^{-1} s^{-1} and (9.78 ± 0.08) × 10^2 L^2 mol^{-2} s^{-1}.[10] This relationship of k_1 with the concentration of imidazole is related to its role as a nucleophilic and basic catalyst (step 1, **Scheme 2**).[10]

$$k_1 = k_{1(2)}[IMI\text{-}H] + k_{1(3)}[IMI\text{-}H]^2 \qquad (3)$$

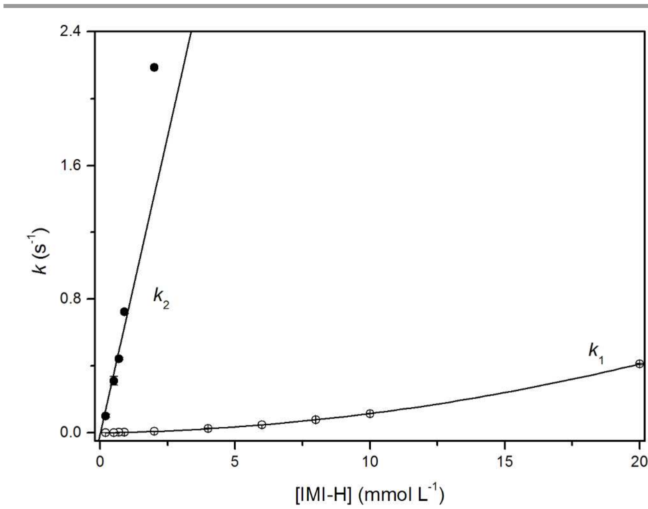

Figure 1. Dependence of the rate constants k_1 (o) and k_2 (●) on imidazole concentration (in EtOAc, at 25 °C, [TCPO] = 0.1 mmol L^{-1}, [H_2O_2] = 10.0 mmol L^{-1}, [**1**] = 1.0 mmol L^{-1}). The k_1 values were fitted using Eq. 3: $k_{1(2)}$ = 2.4 ± 0.1 L mol^{-1} s^{-1} and $k_{1(3)}$ = (9.03 ± 0.05) × 10^2 L^2 mol^{-2} s^{-1}; r^2 = 0.99997. The k_2 values show a linear correlation (Eq. 4): $k_{2(3)}$[H_2O_2] = (7,1 ± 0,5) × 10^2 L mol^{-1} s^{-1}; r = 0.93056. The value at 2.0 mmol L^{-1} was not used on the linear regression of the k_2 data.

This journal is © The Royal Society of Chemistry 2012

Photochemical & Photobiological Sciences Accepted Manuscript

The second step of the PO sequence (step 2, **Scheme 2**) involves H_2O_2 acting as a nucleophile, with basic catalysis by IMI-H,[10] and a first-order dependence of k_2 on both reagents (**Figures 1** and **2**). From the slope of linear plots, corrected by the fixed concentration of $[H_2O_2]$ = 10.0 mmol L^{-1} or [IMI-H] = 1.0 mmol L^{-1}, values were found for the termolecular rate constant $k_{2(3)}$ = 7.1 × 10^4 and 4.3 × 10^4 L^2 mol^{-2} s^{-1}, respectively, from the imidazole (**Figure 1**) and H_2O_2 (**Figure 2**) k_2 dependence. Considering both determinations, a mean value of $k_{2(3)}$ = (6 ± 1) × 10^4 L^2 mol^{-2} s^{-1} is found, which is in agreement with the 2 × 10^4 L^2 mol^{-2} s^{-1} one found previously with DPA as ACT.[10]

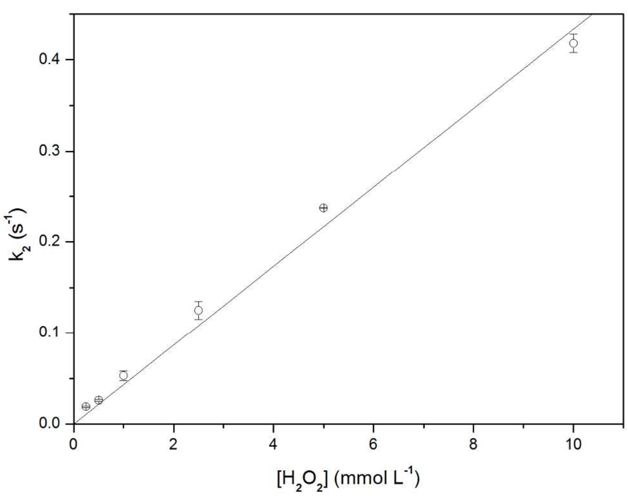

Figure 2. Dependence of the rate constant k_2 on H_2O_2 concentration (in EtOAc, at 25 °C, [TCPO] = 0.1 mmol L^{-1}, [IMI-H] = [**1**] = 1.0 mmol L^{-1}). The k_2 values show a linear correlation (Eq. 4): $k_{2(3)}$[IMI-H] = (4.3 ± 0.1) × 10^1 L mol^{-1} s^{-1}; r = 0.99093.

$$k_2 = k_{2(3)}[IMI\text{-}H][H_2O_2] \qquad (4)$$

Therefore, given that the observed rate constants k_1 and k_2 of the CL-intensity time-profiles do not depend on the [ACT] for **1**–**5**, and that the values for the rate constants $k_{1(2)}$, $k_{1(3)}$ and $k_{2(3)}$ are in agreement with formerly reported values,[10] it can be rationalized that: *(i)* compounds **1**–**5** do not take part on the kinetically observable steps of the PO mechanism, and *(ii)* the same overall mechanism is operating for HEI formation (steps 1 to 3, **Scheme 2**), when these lophine derivatives are used as ACTs, alike commonly used activators such as DPA.[8-10]

Control experiments were conducted to verify if the lophine derivatives **1**–**5** emit light through an oxidation process (**Scheme 1**) that could occur concomitantly to the PO reaction. No light emission was detected on the absence of TCPO, with the system [**1**–**5**] = [IMI-H] = 1.0 mmol L^{-1} and $[H_2O_2]$ = 10.0 mmol L^{-1} (**Figure S3**), therefore, indicating that the classical CL oxidation reaction of these lophine derivatives is negligible on the experimental conditions used. Also, it was verified if compounds **1**–**5** could act as basic catalysts of the PO reaction, since these are all hindered imidazole derivatives. There was no light emission for the system [**1**–**5**] = 1.0 mmol L^{-1}, $[H_2O_2]$ = 10.0 mmol L^{-1} and [TCPO] = 0.1 mmol L^{-1} (**Figure S3**), contrarily to what happens on the system additionally containing IMI-H. Thus, it's reasonable to assume that derivatives **1**–**5** do not act as catalysts of the PO reaction and are not involved on the rate-limiting steps of this CL system.

The chemiexcitation mechanism with lophine derivatives

The CL-intensity time profiles' fitted parameters I_{max}, k_1 and k_2 (**Table S1**) were used to simulate and extrapolate the intensity to zero counts, and to calculate Q – the integrated areas under the light emission curves. Q was used to determine the CL quantum yields (Φ_{CL}, **Table S1**), which in turn were converted to the singlet excited states formation quantum yields (Φ_S, **Table S1**) (see Experimental section). Φ_S is always related to a particular experimental condition (temperature, solvent, concentration of reagents, etc); its relationship to the ACT concentration (**Eq. 5**) can be deduced directly from a simplified kinetic scheme.[8,17]

$$\Phi_S = \Phi_S^{\infty} \frac{k_{CAT}[ACT]}{k_D + k_{CAT}[ACT]} \qquad (5)$$

$$\frac{1}{\Phi_S} = \frac{1}{\Phi_S^{\infty}} + \left(\frac{k_D}{\Phi_S^{\infty} k_{CAT}}\right)\frac{1}{[ACT]} \qquad (6)$$

Besides of being dependent on the unimolecular decomposition rate constant of the HEI (k_D) and on the bimolecular ACT-catalysed reaction rate constant (k_{CAT}), Φ_S is also related to Φ_S^{∞}, which is the singlet excited state formation quantum yield at infinite ACT concentration ([ACT] = ∞). This hypothetical experimental condition is one where every HEI molecule that is formed will be intercepted by one ACT molecule.[8] Therefore, Φ_S^{∞} can be seen as the maximum possible excitation yield of the CL system with that particular ACT, being essentially independent of the rate by which the activator interacts with the HEI. For each derivative **1**–**5**, Φ_S^{∞} was obtained through the linear intercept of a double reciprocal plot 1/Φ_S vs. 1/[ACT] (**Eq. 6**, **Figure 3** and **Table 2**).

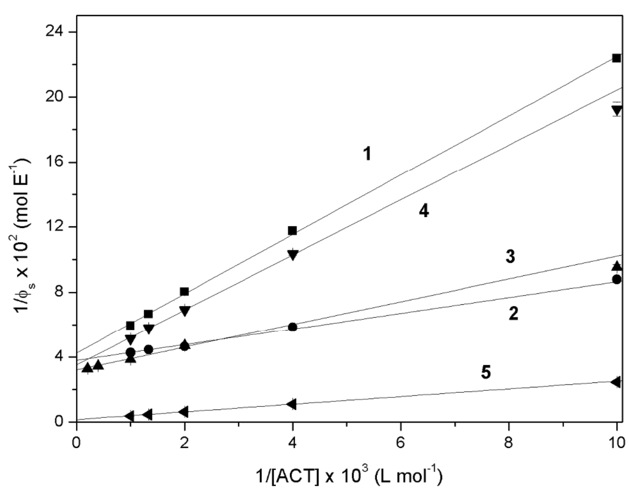

Figure 3. Double reciprocal plots (1/Φ_S vs. 1/[ACT]) for the lophine derivatives **1–5**, used as activators on the imidazole-catalysed reaction of TCPO with H_2O_2.

Photochemical & Photobiological Sciences Accepted Manuscript

Table 2. Chemiluminescence parameters for the imidazole-catalysed reaction of TCPO with H_2O_2, using the lophine derivatives **1**–**5** as activators, together with their half-wave oxidation potentials (E^{ox}).

ACT	E_{ox} (V *vs.* SCE)	$\Phi_S^{\infty} \times 10^3$ (E mol^{-1})	$\Phi_{CL}^{\infty} \times 10^3$ (E mol^{-1})	$k_{CAT}/k_D \times 10^{-3}$ (L mol^{-1})
1	+1.01	2.32 ± 0.05	1.05 ± 0.02	2.36 ± 0.07
2	+0.77	2.67 ± 0.04	1.04 ± 0.01	7.5 ± 0.2
3	+0.88	3.09 ± 0.07	1.14 ± 0.02	5.2 ± 0.2
4	+1.04	2.86 ± 0.08	0.229 ± 0.007	2.07 ± 0.09
5	+1.14	59 ± 3	26 ± 2	0.71 ± 0.05
RUB†	+0.61	680 ± 50	670 ± 50	1.6 ± 0.6
DPA†	+1.06	60 ± 8	57 ± 8	0.34 ± 0.08
ANT†	+1.18	6.9 ± 0.4	1.9 ± 0.1	0.54 ± 0.08

† From Stevani et al.,[8] for the polycondensed aromatic hydrocarbons (PAH) rubrene (RUB), 9,10-diphenylanthracene (DPA) and anthracene (ANT), used as activators. These data were determined in identical experimental conditions ([TCPO] = 0.1 mmol L^{-1}, [IMI-H] = 1.0 mmol L^{-1} and [H_2O_2] = 10.0 mmol L^{-1}, in EtOAc at 25 °C).

From Φ_S^{∞}, values for Φ_{CL} on the same hypothetical condition of [ACT] = ∞ (Φ_{CL}^{∞}) were determined (**Table 2**). The slopes of the double reciprocal plots (**Figure 3**, see **Eq. 6**) were used to determine the ratio k_{CAT}/k_D (**Table 2**), which is a relationship between the ACT-catalysed and unimolecular decomposition rate constants of the HEI. Once that the chemiexcitation process (step 4 in **Scheme 2**) is too fast when compared to the previous steps of the PO reaction (steps 1 to 3, **Scheme 2**),[8,10] a direct measurement of k_{CAT} and k_D is not possible from our kinetic measurements – this can be done only on very specific experimental conditions (see Ciscato *et al.*).[9] Nonetheless, the k_D rate constant is independent of the nature and concentration of the ACT, being related only to the HEI unimolecular decomposition process (**Scheme 3**). Therefore, changes on the k_{CAT}/k_D ratio are actually associated to variations on the k_{CAT} rate constant, due to the bimolecular interaction of the ACT with the HEI (**Scheme 3**).[8]

The obtained data (**Table 2**) can be compared to the results found by Stevani *et al.*,[8] who have worked with the same PO system and on identical experimental conditions. They have used PAH derivatives as activators, such as rubrene (RUB), DPA and anthracene (ANT), which are commonly used ACTs.[7] It can be seen that the k_{CAT}/k_D values for the lophine derivatives **1**–**5** are, on the average, higher than the PAH ones (**Table 2**). RUB, with the lowest oxidation potential (+0.66 V *vs.* SCE, **Table 2**), has a k_{CAT}/k_D ratio lower than those for the most oxidizable lophine derivatives, **2** and **3**, even their E^{ox} values being higher: +0.77 and +0.88 V *vs.* SCE, respectively (**Table 2**).

If an ET process (or at least a charge transfer)[6-9,18] is indeed occurring, one could expect that compounds with lower E^{ox} should have higher k_{CAT} and, therefore, higher k_{CAT}/k_D values. Nonetheless, the value for k_{CAT} includes not only a measurement of the rate constant for the ET process (k_{ET}), but also for the formation of a charge-transfer complex between the ACT and the HEI (K_{CT}), previous to electron transfer (**Eq. 7**, **Scheme 4**).[6,8,18] Steric effects are crucial to determine the magnitude of k_{CAT} in systems where the CIEEL mechanism operates in the chemiexcitation process.[18] It is clearly seen that an increase on the oxidation potential reflects in smaller k_{CAT}/k_D values within the lophine derivatives series (**Table 2**), as expected for the CIEEL mechanism (**Scheme 3**).[6,7]

$$k_{CAT} = K_{CT} k_{ET} \qquad (7)$$

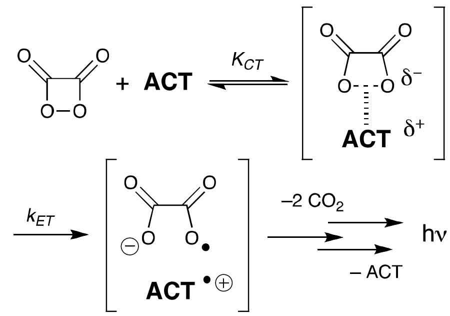

Scheme 4. Formation of the charge transfer complex (K_{CT}) prior to the ET process (k_{ET}), on the sequence that compose the overall k_{CAT} rate constant (Eq. 7). The following steps for light emission generation are not depicted in details; brackets are representing the solvent cavity.[6]

A free-energy correlation between k_{CAT}/k_D and E^{ox} (**Figure 4**) gives a linear relationship (r > 0.97), from which the electron transfer coefficient (α) can be determined, according to the Marcus equation applied for ET processes (**Eq. 8**):[19,20]

$$ln\left(\frac{k_{CAT}}{k_D}\right) = lnA + \alpha B - \left(\frac{\alpha}{RT}\right)E^{ox} \qquad (8)$$

$$with \quad B = \left(\frac{e^2}{R_0 \varepsilon RT} + \frac{E^{red}}{RT}\right)$$

where α is the electron transfer coefficient; R is the universal gas constant (8.21 × 10^{-5} m^3 atm K^{-1} mol^{-1}); T is the temperature (in Kelvin); E^{ox} is the activator oxidation potential, E^{red} is the high-energy intermediate reduction potential (which is constant); e is the electron charge; R_o is the distance between radical ion centers in charge transfer complexes; and ε is the dielectric constant of the solvent.

Such linear free-energy correlation (**Figure 4**) gives a value for α = 0.130 ± 0.003, *i.e.* 0.13, indicating the occurrence of an ET process most likely *via* the CIEEL mechanism (**Scheme 3**).[6] This relatively low value indicates an early transition state regarding the ET and, presumably, the HEI-peroxidic O–O bond cleavage processes, as these two events are supposed to occur concomitantly (**Scheme 4**).[6,20] The α = 0.13 value found here for the PO reaction with lophine derivatives **1**–**5** is in agreement with the ones reported for several CIEEL systems, in the range 0.1–0.3, which includes variations of the PO system[8,9] and the activated decomposition of isolated four-membered strained cyclic peroxides, called 1,2-dioxetanones.[11,18,21]

 This journal is © The Royal Society of Chemistry 2012

Photochemical & Photobiological Sciences Accepted Manuscript

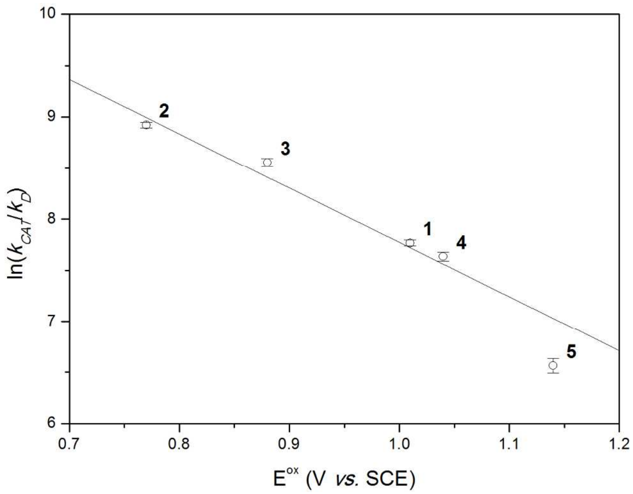

Figure 4. Linear free-energy correlation of the ratio k_{CAT}/k_D with the half-wave oxidation potential (E^{ox}) of lophine derivatives **1–5** (Table 2); intercept = 13.1 ± 0.1, angular coefficient = –5.31 ± 0.15, r = 0.97948.

To the best of our knowledge, the imidazole-catalysed reaction of TCPO with H_2O_2 using RUB as activator is the non-enzymatic system bearing the highest reported emission quantum yield (Φ_{CL}^{∞} = 0.67 E mol^{-1}, **Table 2**).[8,18] The average emission yield Φ_{CL}^{∞} = 1.08 × 10^{-3} E mol^{-1} for compounds **1**–**3** is, respectively, two and one orders of magnitude lower than Φ_{CL}^{∞} for RUB and DPA, being comparable to the yield reported for ANT (**Table 2**). Such overall low Φ_{CL}^{∞} values for **1**–**3**, when compared to the PAH-activated ones, are due to the low Φ_S^{∞} values (**Table 2**) of these systems, given that these derivatives have Φ_{FL} values close to 0.4 (**Table 1**). It has been reported before[10] that imidazole can quench the CL emission of the PO reaction, lowering the emission yields (**Table S2**). Despite of compounds **1**–**5** being imidazole derivatives, no evidences were found that could indicate such quenching action, additionally to their role as ACTs, when in high concentrations up to 10.0 mmol L^{-1}. In this concentration, the observed Φ_S and Φ_{CL} values (**Table S4**) are close to the Φ_S^{∞} and Φ_{CL}^{∞} ones, which, as stated above, can be perceived as the maximum possible excitation and emission yields of the CL system. If a quenching process was supposed to occur in such condition, low values for Φ_S and Φ_{CL} would have been observed.

Table 3. Singlet energy (E_S) of the lophine derivatives **1**–**5** and energy balance for the electron back-transfer process (EBT, Scheme 3).

ACT	E_S † (kJ mol^{-1})	ΔG_{EBT} ‡ (kJ mol^{-1})	ΔG^*_{EBT} § (kJ mol^{-1})
2	340	–333	+7
3	341	–343	–2
1	343	–356	–13
4	340	–359	–19
5	259	–369	–110

† Obtained from the energy gap between the S_0 and S_1 fundamental vibrational states ($\nu_{0\odot 0}$, **Table 1**). ‡ $\Delta G_{EBT} = -F(E_{ox}^{ACT} - E_{red}^{CO2})$, where both E_{ox}^{ACT} (from **Table 2**) and E_{red}^{CO2} = –2,44 V are *vs.* Standard Hydrogen Electrode; *F* is the Faraday constant. § $\Delta G^*_{EBT} = \Delta G_{EBT} + E_S$.

The ten-fold lower Φ_{CL}^{∞} = 2.29 × 10^{-4} E mol^{-1} observed for derivative **4** (**Table 2**) is clearly related to its low fluorescence emission quantum yield (Φ_{FL} = 0.08, **Table 1**), a probable offshoot of the heavy atom effect.[22] Contrarily, the Φ_S^{∞} and Φ_{CL}^{∞} values obtained with derivative **5** are much higher than the ones for **1**–**4**, being comparable to the yields formerly reported for DPA (**Table 2**). Such a higher chemiexcitation yield for **5** can be addressed to the larger accessibility of its electronic excited state, as indicated by the very exergonic ΔG^*_{EBT} = –110 kJ mol^{-1} (**Table 3**), which is the free energy associated with the electron back-transfer process that leads to ACT molecules on the excited state (**Scheme 3**). As discussed elsewhere,[8] Φ_S^{∞} is strongly related to the energy balance involved in the formation of the excited state (i.e., ΔG^*_{EBT}), which, in turn, depends on the energy gap between S_0 and S_1 states (i.e., E_S), and on the free energy associated with the annihilation of the $CO_2^{\bullet-}$ and $ACT^{\bullet+}$ radical ions leading to species on the fundamental state (i.e., ΔG_{EBT}). Thus, the overall low $\Phi_S^{\infty} \approx 3 \times 10^{-3}$ E mol^{-1} chemiexcitation quantum yield for lophine derivatives **1**–**4** is a consequence of the low accessibility of their electronically excited states, since ΔG^*_{EBT} is much less exergonic for these derivatives (**Table 3**).

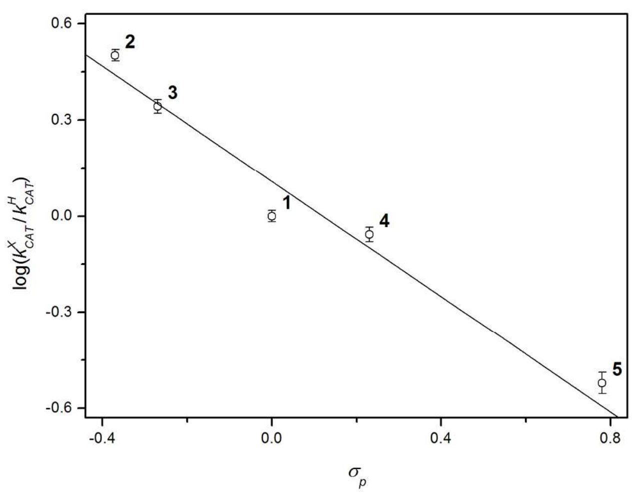

Figure 5 Linear free-energy correlation of the rate constants k_{CAT}^X/k_{CAT}^H for the HEI bimolecular decomposition with the Hammett substituent constants (σ_p); angular coefficient = –0.90 ± 0.03, r = 0.97314.

Hammett plot for the PO reaction with lophine derivatives

Information regarding the build up of charge in the transition state of the chemiexcitation step of CL reactions can be obtained through Hammett plots.[23] However, this is not the case for the PO reaction with commonly used ACTs, such as RUB, DPA and ANT, which vary drastically in structure. Since the lophine derivatives **1**–**5** are different only on a substituent attached to the aryl-imidazolic system, this enables a linear free-energy correlation of the rate constants k_{CAT}^X/k_{CAT}^H – obtained through the k_{CAT}/k_D values (**Table 2**) – with the Hammett substituent constants (σ_p). Such plot (**Figure 5**) shows a good linear dependence (r > 0.97) with ρ = –0.90 ± 0.03. The negative sign of the parameter ρ indicates the formation of a

Photochemical & Photobiological Sciences Accepted Manuscript

partial positive charge in the transition state of the rate-determining step – namely, the electron transfer from the ACT to the HEI on the chemiexcitation pathway, with formation of $ACT^{+\bullet}$, as predicted by the CIEEL sequence (**Schemes 3** and **4**). Even k_{CAT} being composed by K_{CT} and k_{ET} (**Eq. 7**), it can be stated that the influence of the substituent is mainly on the ET process, since a ρ value close to unity indicates that this bimolecular reaction is as sensitive to the substituent as benzoic acid. It can be assumed that the electronic effect of the substituents on the imidazole moiety, where the electron density is probably higher in these lophine derivatives, is basically electron-withdrawing inductive (–I). Thus, there is no direct evidence for the resonance between the imidazolic and arylic groups of these molecules, in analogy to the rationalization applied in Hammett's model system, concerning the acidity of benzoic acid derivatives.

Conclusions

This work has addressed the use of lophine derivatives **1**–**5** as ACTs of the chemiluminescent PO reaction. Kinetic evidences have shown that such compounds do not act on the slow steps of the reaction, regarding the formation of the HEI. Alike commonly used ACTs, lophines **1**–**5** act only on the chemiexcitation step, which occurs through the CIEEL mechanism. Average low excited state formation and emission quantum yields ($\approx 10^{-3}$ E mol^{-1}) were observed, except for derivative **5**, which showed yields ten fold higher. The use of linear free-energy correlations provided evidences not only for an electron transfer, but also for the formation of a partial positive charge on the ACT during the chemiexcitation step, as expected for the CIEEL sequence (**Scheme 3**).

Acknowledgements

We thank the Fundação de Amparo à Pesquisa do Estado de São Paulo (FAPESP; JA 2013/17332-6, TLF 2011/17587-9, LFMLC 2012/02428-5 and FHB 2012/13807-7) and the Coordenação de Aperfeiçoamento de Pessoal de Nível Superior (CAPES) for financial support.

Notes and references

[a] Centro de Ciências Naturais e Humanas, Universidade Federal do ABC, Santo André, SP, Brazil. E-mail: fernando.bartoloni@ufabc.edu.br. Fax: +55 11 49960090. Tel.: +55 11 49968375.
[b] Instituto de Ciências Ambientais, Químicas e Farmacêuticas, Universidade Federal de São Paulo, Diadema, SP, Brazil.
Electronic Supplementary Information (ESI) available: spectrophotometric data (Figures S1 and S2), chemiluminescence emission time-profiles (Figure S3) and spectrum (Figure S4), and emission kinetics data (Tables S1–S3). See DOI: 10.1039/b000000x/

1 B. Radziszewski, Ueber die Constitution des Lophins und verwandter Verbindungen, *Ber. Chem. Ges.*, 1877, **10**, 70.
2 G. Lu, J. Wada, T. Kimoto, H. Iga, H. Nishigawa, M. Kimura, Z. Z. Hu, The Chemiexcitation of the Chemiluminescence of Lophine Peroxide Anions via a Partially Cyclic Transition State, *Eur. J. Org. Chem.*, 2014, 1212; M. Kimura, G. H. Lu, H. Nishigawa, Z. Q. Zhang, Z. Z. Hu, Singlet oxygen generation from lophine hydroperoxides, *Luminescence*, 2007, **22**, 72; M. Tsunenaga, H. Iga, M. Kimura, Location effect of an OH group on the chemiluminescence efficiency of 4-hydroperoxy-2-(*o*-, *m*-, or *p*-hydroxyphenyl)-4,5-diphenyl-4*H*-isoimidazoles, *Tetrahedron Lett.*, 2005, **46**, 1877; M. Kimura, H. Nishikawa, H. Kura, H. Lim, E. H. White, Maximization of the Chemiluminescence Efficiency of 1,4,5-Triarylhydroperoxy-4*H*-isoimidazoles, *Chem. Lett.*, 1993, 505; E. H. White, M. J. C. Harding, Chemiluminescence in liquid solutions: the chemiluminescence of lophine and its derivatives, *Photochem. Photobiol. Sci.*, 1965, **4**, 1129; White, M. J. C. Harding, The chemiluminescence of lophine and its derivatives, *J. Am. Chem. Soc.*, 1964, **86**, 5686; T. Hayashi, K. Maeda, Mechanism of chemiluminescence of 2,4,5-triphenylimidazole, *Bull. Chem. Soc. Jap.*, 1962, **35**, 2057.
3 K. Nakashima, Lophine derivatives as versatile analytical tools, *Biomed. Chromatogr.*, 2003, **17**, 83.
4 N. Kuroda, R. Shimoda, M. Wada, K. Nakashi, Lophine derivatives and analogues as new phenolic enhancers for the luminol–hydrogen peroxide–horseradish peroxidase chemiluminescence system, *Anal. Chim Acta*, 2000, **403**, 131.
5 L. F. M. L. Ciscato, F. A. Augusto, D. Weiss, F. H. Bartoloni, S. Albrecht, H. Brandl, T. Zimmermann, W. J. Baader, The chemiluminescent peroxyoxalate system: state of the art almost 50 years from its discovery, *ARKIVOC*, 2012, **iii**, 391; F. H. Bartoloni, L. F. M. L. Ciscato, M. M. M. Peixoto, A. P. F. Santos, C. S. Santos, S. Oliveira, F. A. Augusto, A. P. E. Pagano, W. J. Baader, Light: a rare reaction product, *Quim. Nova*, 2011, **34**, 544.
6 W. J. Baader, C. V. Stevani, E. L. Bastos, Chemiluminescence of Organic Peroxides, in *The Chemistry of Peroxides*, ed. Z. Rappoport, John Wiley & Sons, Chichester, 2006, vol. 2, pp. 1211.
7 F. A. Augusto, G. A. de Souza, S. P. de Souza Jr., M. Khalid, W. J. Baader, Efficiency of Electron Transfer Initiated Chemiluminescence, *Photochem. Photobiol.*, 2013, **89**, 1299.
8 C. V. Stevani, S. M. da Silva, W. J. Baader, Studies on the mechanism of the excitation step in peroxyoxalate chemiluminescence, *Eur. J. Org. Chem.*, 2000, 4037.
9 F. H. Bartoloni, L. F. M. L. Ciscato, F. A. Augusto, W. J. Baader, Inverse electron transfer in peroxyoxalate chemiexcitation using easily reducible activators, *Quim. Nova*, 2010, **33**, 2055; L. F. M. L. Ciscato, F. H. Bartoloni, E. L. Bastos, W. J. Baader, Direct Kinetic Observation of the Chemiexcitation Step in Peroxyoxalate Chemiluminescence, *J. Org. Chem.*, 2009, **74**, 8974; S. M. Silva, K. Wagner, D. Weiss, R. Beckert, W. J. Baader, Studies on the chemiexcitation step in peroxyoxalate chemiluminescence using steroid-substituted activators, *Luminescence*, 2002, **17**, 362; C. L. R. Catherall, T. F. Palmer, R. B. Cundall, Chemiluminescence from reactions of bis(pentachlorophenyl)oxalate, hydrogen peroxide and fluorescent compounds. Kinetics and mechanism., *J. Chem. Soc., Faraday Trans. 2*, 1984, **80**, 823.
10 S. M. da Silva, F. Casallanovo, K. Oyamaguchi, L. F. M. L. Ciscato, C. V. Stevani, W. J. Baader, Kinetic studies on the peroxyoxalate chemiluminescence reaction: determination of the cyclization rate constant, *Luminescence*, 2002, **17**, 313; C. V. Stevani, D. F. Lima, V.

This journal is © The Royal Society of Chemistry 2012
Photochemical & Photobiological Sciences Accepted Manuscript

G. Toscano, W. J. Baader, Kinetic studies on the peroxyoxalate chemiluminescent reaction: imidazole as a nucleophilic catalyst, *J. Chem. Soc., Perkin Trans. 2*, 1996, 989.

11 G. B. Schuster, Chemiluminescence of organic peroxides. Conversion of ground-state reactants to excited-state products by the chemically initiated electron-exchange luminescence mechanism, *Acc. Chem. Res.*, 1979, **12**, 366; G. B. Schuster, S. P. Schmidt, Chemiluminescence of organic compounds, *Adv. Phys. Org. Chem.*, 1982, **18**, 187.

12 M. L. Cotton, H. B. Dunford, Studies on horseradish peroxidase. XI. On the nature of compounds I and II as determined from the kinetics of the oxidation of ferrocyanide, *Can. J. Chem.*, 1973, **5**, 582.

13 L. Benisvy, A. J. Blake, D. Collison, E. S. Davies, C. D. Garner, E. J. L. McInnes, J. McMaster, G. Whittaker, C. Wilson, A phenol-imidazole pro-ligand that can exist as a phenoxyl radical, alone and when complexed to copper (II) and zinc (II), *Dalton Trans.* 2003, 1975.

14 S. L. Murov, I. Carmichael, G. L. Hug, *Handbook of Photochemistry*, 2nd ed., Marcel Decker Inc.: New York, 1993.

15 J. Lee, A. S. Wesley, J. F. Ferguson III, H. H. Seliger, The use of luminol as a standard of photon emission, *in Bioluminescence in Progress*, eds. F. H. Johnson and Y. Haneda, Princeton University Press, Princeton, 1965, pp. 35.

16 A. MacDonald, K. W. Chan, T. A. Nieman, Lophine chemiluminescence for metal ion determinations, *Anal. Chem.*, 1979, **51**, 2077.

17 C. V. Stevani, Ph.D. Thesis, Universidade de São Paulo, 1997.

18 M. A. de Oliveira, F. H. Bartoloni, F. A. Augusto, L. F. M. L. Ciscato, E. L. Bastos, W. J. Baader, Revision of Singlet Quantum Yields in the Catalyzed Decomposition of Cyclic Peroxides, *J. Org. Chem.*, 2012, **77**, 10537; L. F. M. L. Ciscato, F. H. Bartoloni, A. S. Colavite, D. Weiss, R. Beckert, S. Schramm, Evidence supporting a 1,2-dioxetanone as an intermediate in the benzofuran-2(3*H*)-one chemiluminescence, *Photochem. Photobiol. Sci.*, 2014, **13**, 32.

19 R. A. Marcus, Chemical and electrochemical electron-transfer theory, *Annu. Rev. Phys. Chem.*, 1964, **15**, 155.

20 F. Scandola, V. Balzani, G. B. Schuster, Free-energy relationships for reversible and irreversible electron-transfer processes, *J. Am. Chem. Soc.*, 1981, **103**, 2519.

21 *Chemical and Biological Generation of Excited States*, eds. W. Adam and G. Cilento, Academic Press, New York, 1982; J. P. Smith, A. K. Shrock, G. B. Schuster, Chemiluminescence of organic peroxides. Thermal generation of an *o*-xylylene peroxide, *J. Am. Chem. Soc.*, 1982, **104**, 1041; M. J. Darmon, G. B. Schuster, Thermal chemistry of cyclopropyl-substituted malonyl peroxides. A new chemiluminescent reaction, *J. Org. Chem.*, 1982, **47**, 4658; S. P. Schmidt, G. B. Schuster, Chemiluminescence of dimethyldioxetanone. Unimolecular generation of excited singlet and triplet acetone. Chemically initiated electron-exchange luminescence, the primary light generating reaction, *J. Am. Chem. Soc.*, 1980, **102**, 306; B. G. Dixon, G. B. Schuster, Investigation of the mechanism of the unimolecular and the electron-donor-catalyzed thermal fragmentation of secondary peroxy esters. Chemiluminescence of 1-phenylethyl peroxyacetate by the chemically initiated electron-exchange luminescence mechanism, *J. Am. Chem. Soc.*, 1979, **101**, 3116; J.-Y. Koo, G. B. Schuster, Chemiluminescence of diphenoyl peroxide - chemically-initiated electron exchange luminescence - new general mechanism for chemical production of electronically excited-states, *J. Am. Chem. Soc.*, 1978, **100**, 4496.

22 W. Adam, Determination of chemiexcitation yields in the thermal generation of electronic excitation from 1,2-dioxetanes, in *Chemical and Biological Generation of Excited States*, eds. W. Adam and G. Cilento, Academic Press, New York, 1982, pp. 115; T. Wilson, *Int. Rev. Sci. Phys. Chem. Ser. Two*, 1976, **9**, 266.

23 L. F. M. L. Ciscato, F. H. Bartoloni, D. Weiss, R. Beckert, W. J. Baader, Experimental Evidence of the Occurrence of Intramolecular Electron Transfer in Catalyzed 1,2-Dioxetane Decomposition, *J. Org. Chem.*, 2010, **75**, 6574.

Photochemical & Photobiological Sciences Accepted Manuscript

"Lophine derivatives as activators in peroxyoxalate chemiluminescence"

J. Alves, A. Boaro, J. S. da Silva, T. L. Ferreira, V. B. Keslarek, C. A. Cabral, R. B. Orfão Jr.,

L. F. M. L. Ciscato and F. H. Bartoloni.

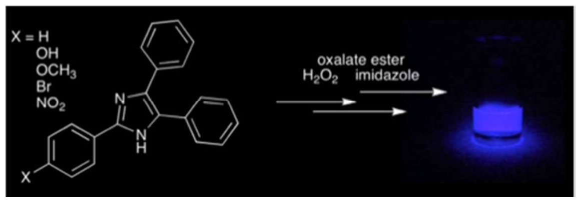

Lophine and four of its derivatives were applied, for the first time, as activators of the chemiluminescent peroxyoxalate reaction.

Photochemical & Photobiological Sciences Accepted Manuscript